THE JOURNAL OF PHYSICAL CHEMISTRY B

Article

pubs.acs.org/JPCB

Unusual Optical Resolution of All Four Tryptophan Residues in MPT63 Protein by Phosphorescence Spectroscopy: Assignment and Significance

Ranendu Ghosh,[†] Manini Mukherjee,[‡] Krishnananda Chattopadhyay,[†,*] and Sanjib Ghosh[‡,*]

[†]Structural Biology & Bio-Informatics Division, Indian Institute of Chemical Biology, Kolkata-700 032, India

[‡]Department of Chemistry, Presidency University, Kolkata 700 073, India

ABSTRACT: MPT63, a secreted protein of unknown function that is specific to *Mycobacterium tuberculosis* and a potential drug target, contains four Tryptophan (Trp/W) residues located at positions 26, 48, 82, and 129 in the amino acid sequence. All of the four Trp residues have been optically resolved by simple inexpensive phosphorescence spectroscopy at 77 K. The protein architecture provides a delicate micro-environment and location of Trp residues giving rise to four different (0,0) bands in the phosphorescence spectra. Calculation of intra Trp energy transfer (ET) efficiency, accessible surface area (ASA) of Trp residues, and environment of Trp in the wild-type (WT) and the mutant W26F [where, Trp 26 is replaced by phenyl alanine (Phe/F)] reveal: E_{T1} (W82) > E_{T1} (W48) > E_{T1} (W129) > E_{T1} (W26), where E_{T1} is the lowest ($\pi-\pi^*$) triplet state energy of Trp. The (0,0) band observed at 421.6 nm assigned for Trp 26 is found to be the longest wavelength (0,0) band so far reported in the literature. Fluorescence in WT and W26F is dominated by buried or partially exposed Trp residues indicated by time-resolved spectra. Circular Dichroism (CD) studies and the time-resolved anisotropy measurement confirm the unaltered secondary and tertiary structure of the mutant compared to that of the WT. Excitation energy dependent phosphorescence spectra suggest that the intensity of the different (0,0) bands could be tuned and Tyrosine (Tyr/Y) residue is silent in emission . Optical resolution of all the Trp residues will help understand the role of each Trp residue in the folding/unfolding mechanism and in the interaction with other systems.

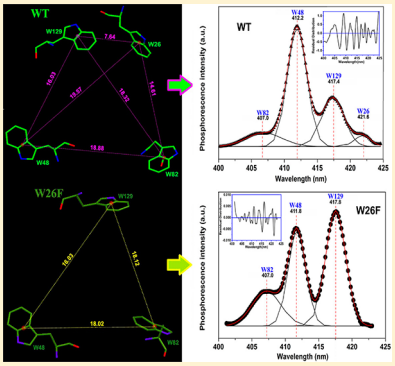

1. INTRODUCTION

Several structural aspects including conformational variation as well as folding/unfolding phenomenon in proteins are often characterized by steady state and time-resolved fluorescence of Trp residue that acts as the intrinsic probe. Trp fluorescence, using selective excitation, along with steady state and time-resolved anisotropy studies of proteins and complexes of proteins with other molecules (nucleic acid, proteins, suitable ligands, as drug or toxic molecule) are widely used for both structural and dynamical information. However, it is difficult to ascertain the microenvironment of each Trp residue and its contribution in a multi Trp protein to the total fluorescence. This is due to the fact that the fluorescence spectra are usually broad and even a protein containing a single Trp residue exhibits multiexponential fluorescence decay. A wavelength selected Stern−Volmer plot of fluorescence quenching using various quenchers has been used to partially resolve steady state emission spectra into components.[1] Although decay associated spectra (DAS) and time-resolved emission spectra (TRES) using time-resolved data at various wavelength could be helpful in some cases, uncertainties and other complications primarily arising from the contributions of other Trp residues could not be ruled out.[2] This problem is overcome in many cases by using mutated proteins where one or more Trp is/are replaced by either Tyr or Phe.

Although the fluorescence behavior of Trp residues are poorly resolved and broad, low temperature phosphorescence (LTP) spectra of Trp in proteins in suitable cyrosolvent exhibit well-defined structured spectra with defined (0,0) and other vibronic bands. The narrowness of the (0,0) bands of phosphorescence spectra at 77 K is attributed to the smaller excited state dipole moment of the lowest triplet state.[3] The position and the width of the (0,0) vibronic band, the lifetime of the lowest triplet state of Trp and the overall structure of the phosphorescence spectra are characteristic of the immediate environment of the Trp, e.g., polarity, polarizability, heterogeneity, and solvent accessibility.

Studies of the LTP of Trp residues in proteins have revealed a opposite Stokes shift pattern for the lowest triplet state with respect to the lowest singlet state.[4−9] The blue-shifted phosphorescence, typical of a free Trp in a polar solvent, can be attributed to the lower polarizability of the environment and to the poor stabilization of the triplet state by rigid solvation geometry that is organized to effectively stabilize the ground state by dipole−dipole alignment. The red-shifted (0,0) band however, is characteristic of a Trp residue located in a buried polarizable environment that stabilizes the triplet state more

Received: July 30, 2012
Revised: September 19, 2012
Published: September 21, 2012

than the ground state.[3,10,11] Rigidity and immediate local charges also control the position and the width of the (0,0) band. Specific interactions with polar residues can result in blue-shifted origins for buried Trp residues, for example a single Trp residue in Rnase T1.[10,5]

Proteins containing more than one Trp residue generally exhibit a single (0,0) band in their phosphorescence spectra.[3] The absence of overlapping phosphorescence spectra with multiple (0,0) bands may occur due to several factors. These include (i) energy transfer (ET) to another residue, (ii) interaction with neighboring residue through the formation of charge-transfer complex, (iii) electron transfer from the excited state, and (iv) intrinsic quenching of the Trp residue by a neighboring residue like Cysteine, Histidine, or Disulfide bridge.[13−15] Photoinduced electron transfer quenching from excited state of indole to the disulfide and temperature dependence of disulfide quenching of the Trp phosphorescence of Lysozyme and α-bungarotoxin have been demonstrated.[15]However, there are exceptions and several multi-Trp proteins have been shown to exhibit overlapping phosphorescence spectra with definite multiple (0,0) bands corresponding to different Trp residues present in the protein.[4,10,12−35] The observation of multiple (0,0) bands is usually possible when the Trp residues in a protein are in widely different environments and photoinduced energy transfer among the emitting Trp residues is prevented.

Multiple (0,0) bands have been observed in Horse Liver Alcohol Dehydrogenase (HLAD) (two out of two Trps),[4]Al-Allergen Ra5 of the pollen of *Ambrosia elaitor* (two out of two Trps),[17] glyceraldehyde 3-phosphate dehydrogenase (GAPD) (two out of three for yeast and rabbit and all the three for yeast),[18,19] bacteriophage T4 lysozyme (two out of three Trps),[20−23] Actin from Rabbit Muscle (two out of four Trps),[24,25] *E. coli.* Asparate aminotransferase (three out of five Trps),[26] Yeast Phosphoglycerate kinase (two out of two Trps),[27] *E. coli*. Trp repressor (two out of two Trps),[28] *E. coli* Mannitol Transporter (two out of four Trps),[29] *E. coli* Alkaline Phosphatase (AP) (two out of three Trps),[12−14] D-galactose/D-glucose-binding protein (GGBP) from *E. coli.* (two out of five Trps),[30] Human placental ribonuclease inhibitor (hRI) (two out of six Trps),[31] Human Erythropoietin (two out of three Trps),[32] bovine Vertebrate odorant-binding proteins ObP (two out of two Trps),[33] Esterase from *Pseudoalteromonas haloplanktis* (two out of four Trps).[34] An anomalous blue-shifted (0,0) band was obtained at 402.0 nm in modified bovine serum albumin (BSA) with bound fatty acids removed.[35]BSA having two Trp residues at 134 and 213, usually exhibits a single (0,0) band at 412.0 nm arising from Trp 213.[35]

Assignments of the (0,0) vibronic band to a particular Trp residue are made either by using suitably mutated proteins or using the crystal structure data of the native proteins or both. Crystal structure data provide the degree of solvent exposure and the nature of residues in the immediate vicinity Trp residue. In some cases, functional aspects of the protein have also been considered to support the assignment. In the case of *E. coli* AP, the phosphorescence band corresponding to Trp 109 has been assigned using photo induced energy transfer study in Tb-AP, where all the Zn^{2+} and Mg^{2+} ions in AP are replaced by Tb^{3+}.[12,13] A somewhat anomalous result was obtained only in the case of *E. coli* Trp repressor containing two Trp residues at 19 and 99. Trp 99 exhibits a red-shifted phosphorescence (0,0) bands compared to that of Trp 19.[28] Phosphorescence and Optical Detection of Magnetic Resonance (ODMR) data are indicative of a typical interior residue of Trp 99 compared to that of Trp 19. However, fluorescence data indicate Trp 99 to be relatively solvent exposed compared to Trp 19. These opposing results have been explained either due to polarizability or polarity of residues around the indole rings or a change in protein conformation upon freezing, which creates the somewhat buried and less solvent exposed environment of Trp 99.[28]

The present study reports an extensive investigation of phosphorescence spectroscopy with a protein MPT63, which contains four Trp residues at positions 26, 48, 82, and 129. MPT63 is chosen as the model because of its importance in both biological and structural studies. It is a secreted protein of unknown function that is specific to *Mycobacterium tuberculosis* (*M. tuberculosis*) which might be a potential drug target.[36] Tuberculosis (TB) is caused by the bacterial pathogen *M. tuberculosis*, which kills more than millions of people around the world every year.[36] Secreted proteins like MPT63 are often needed for bacteria to survive in a hostile environment or to successfully colonize a host. The protein has been shown to stimulate humoral immune responses in guinea pigs infected with a virulent strain.[37] WT MPT63 having an apparent molecular weight of 17.5 KD[37] is a predominantly β-sheet rich protein.[36]The X-ray crystal structure of MPT63 at 1.5 Å resolution (Figure 1) has been solved. The protein has been found to be a β-sandwich containing an immunoglobulin-like fold. The protein composed of two antiparallel β-sheets differing in lengths juxtaposed to each other and a small 3_{10}

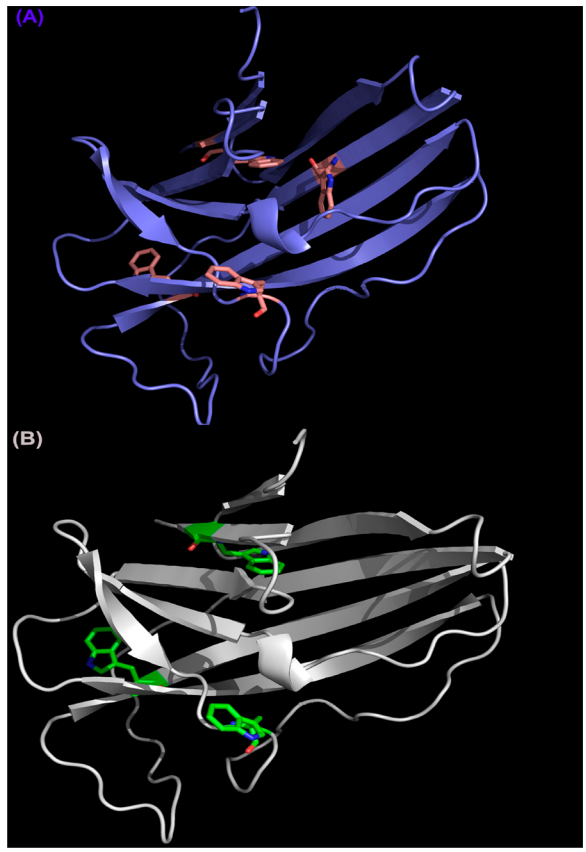

Figure 1. Cartoon representation of (A)WT and (B)W26F *Mycobacterium tuberculosis* MPT63 protein (WT PDB ID code 1 LMI). Tryptophan residues (Trp26, Trp48, Trp82, and Trp129) are shown in sticks. The structure is generated by PyMol.

helix. The longer sheet contains four anti-parallel β-strands and the shorter sheet made up of five β-strands and the helix.

The present work reports room temperature steady state and time-resolved fluorescence with major emphasis on steady state and time-resolved LTP at 77 K in 40% ethylene glycol (EG) glassy matrix. The LTP reveals that four out of four Trp residues are optically resolved. The assignment of the different (0,0) bands to different Trp residues have been achieved by (i) the LTP of a mutated MPT63, where Trp 26 has been replaced by Phe (W26F) and (ii) a detail calculation of intramolecular ET between all Trp pairs considering both the ^1L_a and ^1L_b[38] bands of Trp using the crystal structure data for WT and the data obtained from the predicted structure of the mutant. The predicted structure of the W26F mutant has been obtained using computational analysis.

LTP of the WT and the W26F mutant at different excitation wavelength (λ_{exc}) has been carried out to obtain the comparative picture of the environment of each of the four Trp residues and a possibility of selective excitation of Trp residue. Far UV CD has been used to monitor if there is any secondary structural difference between WT and W26F mutant. Steady state and time-resolved fluorescence spectroscopy of both the WT and the mutants have been carried out to obtain a comparative photophysical behavior of the wild type and the mutant protein. Time resolved anisotropy measurement in WT and W26F mutant has also been carried out to further characterize the hydrodynamics of the wild type and mutant proteins.

This is the first time that a protein containing four Trp residues has been shown to exhibit four distinct optically resolved (0,0) bands using a simple inexpensive LTP. The longest wavelength phosphorescence (0,0) band observed for MPT63 at 421.6 nm has been assigned to residue Trp 26. This is the lowest energy (0,0) band so far reported in the literature. The lowest energy (0,0) band reported to date is at 420.0 nm for Trp 310 in yeast GAPD,[19] whereas the highest energy (0,0) band was observed at 402.0 nm for modified BSA.[35] Allergen Ra5 of the pollen of *Ambrosia elaitor* containing two Trp residues was found to exhibit two (0,0) bands at 403.0 nm and 409.5 nm.[17] The Trp residue showing (0,0) band at 403.0 nm was suggested to be stabilized by a strong polar interaction involving a charged group in a neighboring residue.[17]Since all of the four Trp residues are optically resolved, this study will help us to understand the role of each Trp residue in MPT63 in the folding/unfolding process, the characterization of possible rotamers at various pH and the function of each Trp in the interaction of the protein with other systems without using any mutated variety.

2. EXPERIMENTAL SECTION

2.1. Materials: Preparation of WT and W26F MPT63. *2.1.1. Plasmids, Bacterial Strains, And Site-Directed Mutagenesis.* The plasmid pQE30 containing the wild type MPT63 gene was kindly provided by Dr. David Eisenberg (University of California, Los Angeles, U.S.). Plasmids were transformed in *E. coli* XL1-Blue cells. Site-directed mutagenesis (W26F) was carried out using a QuickChange site-directed mutagenesis kit (Stratagene). The mutation was verified by DNA sequencing of the entire mutant MPT 63 (W26F) gene.

2.1.2. Expression and Purification of MPT63. Single colonies from transformed strains were used to express and purify the protein. XL1-Blue cells containing the wild type (WT) and mutant (W26F) MPT 63 plasmids were grown aerobically at 37 °C in an LB medium containing 100 μg/mL ampicillin and induced with 1 mM IPTG for 4 h when the O.D. was 0.5 at 600 nm. Cells were harvested by centrifugation at 8000 rpm for 15 min at 4 °C and resuspended in 40 mL of sonication buffer (50 mM Potassium phosphate, 300 mM KCl, 10 mM imidazole, pH 7.8). Cells were subjected to one cycle of freezing-thawing and then lysed by sonication. Prior to sonication 1 mM phenylmethylsulfonyl fluoride (PMSF) was added to the sonication buffer. Cell lysates were centrifuged at 12 500 rpm for 45 min at 4 °C. Purification of N-terminal six histidine tagged recombinant MPT63 (recMPT63) by nickel-affinity chromatography were performed as recommended by Qiagen. Supernatants were mixed with 2 mL of Ni-agarose resin (Qiagen), previously equilibrated in sonication buffer, and stirred at 4 °C for 1 h. The protein and resin slurry were then loaded into a column and washed with 10 volumes of sonication buffer followed by 10 volumes of wash buffer (50 mM potassium phosphate K_3PO_4, 300 mM KCl, 20 mM imidazole, pH 7.8). Protein was eluted in the same buffer with a gradient of 20 to 500 mM imidazole. Fractions containing the protein were pooled and were dialyzed overnight against mono-Q start buffer (30 mM Tris-HCl, 100 mM KCl, pH 8.7) and then applied to a monoQ FPLC column pre-equilibrated in the same buffer (30 mM Tris-HCl, 100 mM KCl, pH 8.7). The column was washed with 20 volumes of the same buffer, and the protein was eluted with a 100 to 500 mM KCl gradient. Fractions containing purified protein as assessed by SDS-PAGE (purity >90%), recombinant proteins were pooled and dialyzed against 20 mM Sodium phosphate buffer ph 7.4 and aliquots were stored at −20 °C until required. The concentrations of wild type (WT) and mutant (W26F) MPT 63 were determined using BCA analysis kit.

2.2. Instrumentation. *2.2.1. Circular Dichroism (CD) Measurements.* CD spectroscopic studies were carried out using a Jasco J715 spectropolarimeter (Japan Spectroscopic Ltd.). Far-UV CD spectra (between 200 and 250 nm) were recorded with 1 μM protein in 20 mM sodium phosphate buffer pH 7.5 using a cuvette with a path length of 0.1 cm. Five consecutive scans were accumulated and the average spectra were recorded.

2.2.2. Steady State Fluorescence Measurements. UV−vis absorption spectra were recorded on a Hitachi U-4100 UV−vis-NIR spectrophotometer at 298 K. The steady state emission measurements of 1 μM WT and W26F MPT63 were carried out using a Hitachi Model F-7000 spectrofluorimeter equipped with a 150-W xenon lamp, at 298 K using a stopper cell of 0.5 cm path length. The emission measurements of 1 μM WT and W26F MPT63 were made by exciting the samples at 280 and 295 nm (in order to minimize the contribution from Tyr) using the correct mode of the instrument. Quantum yield (φ) of WT and W26F MPT63 was determined using the procedure described earlier.[39] In both, the measurement excitation and emission band passes were 10 and 5 nm. Inner filter effects have been eliminated in all of the emission spectra.

2.2.3. Low Temperature Phosphorescence Measurement. Emission studies at 77 K were made using a Dewar system having a 5 mm o.d. quartz tube. The freezing of the samples at 77 K were done at the same rate for all of the samples. Phosphorescence was measured in a Hitachi F-7000 spectrofluorimeter equipped with phosphorescence accessories. All of the samples were made in 40% EG for measurements at 77 K. The samples were excited at different wavelengths (270−305 nm) using a 10 nm band-pass, and the emission band-pass was

1 nm except with λ_{exc} = 305 nm, where the emission band-pass was 2.5 nm.

2.2.4. Time Resolved Emission Measurement. Singlet state lifetime (τ) was measured by Time Master fluorimeter from Photon Technology International (PTI, U.S.).The system consists of a pulsed laser driver of a PDL series i.e., PDL-800-B (from Picoquant, Germany) with interchangeable sub nano second pulsed LEDs and pico-diode lasers (Picoquant, Germany) with a TCSPC set up (PTI, U.S.).The software Felix 32 controls all acquisition modes and data analysis of the Time Master system.[40] Decay measurement using "magic angle" detection with an emission polarizer set at 55° were carried out and no detectable difference in the fitted τ values with those obtained from normal decay measurements were observed. The sample of 1 μM WT and W26F MPT63 were excited using PLS-290(Pulse Width-700 ps) at a repetition frequency 10 MHz. Instrument response functions (IRF) were measured at the respective excitation wavelengths, namely, 290 nm using slits with a band-pass of 3 nm using Ludox as the scatterer. The decay of sample was analyzed by a nonlinear iterative fitting procedure based on the Marquardt algorithm. The deconvolution technique used can determine the lifetime up to 200 ps with sub nano second pulsed LEDs. The quality of fit has been assessed over the entire decay, including the rising edge, and tested with a plot of weighted residuals and other statistical parameters, for example, the reduced χ^2 ratio and the Durbin-Watson (DW) parameters.[40]

The decay times in the milliseconds or longer range were measured by a phosphorescence time-based acquisition mode of the QM-30 from PTI, U.S. in which emission intensity is measured as a function of time. The decay parameters were recovered using a nonlinear iterative fitting procedure based on the Marquardt algorithm.

Anisotropy decay measurement was also carried out in Time Master Fluorimeter (PTI, U.S.) using PLS-290 and motorized Glen Thompson polarizer. The anisotropy, $r(t)$, is defined as follows:

$$r(t) = [I_{VV}(t) - G^*I_{VH}(t)]/[I_{VV}(t) + 2G^*I_{VH}(t)] \quad (1)$$

where the $I(t)$ terms are defined as the intensity decay of emission of protein with excitation polarizer orientated vertically and the emission polarizer oriented vertically and horizontally, respectively:

$$G = I_{HV}(t)/I_{HH}(t) \quad (2)$$

where G is the correction term for the relative throughput of each polarization through the emission optics. The entire data analysis was done with the software Felix 32 which analyses the raw data I_{VV} and I_{VH} simultaneously by a global multi-exponential program and then the deconvolved curves (ID_{VV} and ID_{VH}) are used to construct $r(t)$[40] and from the fitted curve the correlation time (θ_C) can be recovered.

2.2.5. Theoretical Calculation. PyMOL 1.5.0.4 (Schrodinger LLC) was used to visualize the conformation of WT and W26F MPT63.[41] It has also been used to measure the distances and the angles between the different residues and to find the surrounding residues around 5 Å of every atom of a particular residue of the protein.[41] Predicted crystal structure of the W26F mutant protein was generated by using DISCOVERY STUDIO version 1.6 (Accelrys Software Inc.). The ASA of WT and W26F MPT63 were calculated using NACCESS.[42]

3. RESULTS AND DISCUSSION

3.1. Far UV CD Spectroscopy with WT and W26F Mutant of MPT63. The far UV CD spectra of the WT and W26F mutant MPT 63 have been shown in Figure 2. The far UV CD spectrum of the WT has a characteristic negative peak at around 216 nm, which is in accordance with the overall β-sheet structure of the protein.[36] The observation of a peak at around 231 nm has also been shown in other protein systems and it is generally assumed to be caused by the tertiary interaction of the aromatic residues inside the hydrophobic core.[43,44] Our data support this hypothesis because the peak at 231 nm has been found to be absent in the W26F mutant (Figure 2). The data further suggest that Trp 26 has major (if not sole) contribution to the CD peak at 231 nm. The data also give preliminary evidence that Trp 26 is located inside the hydrophobic core. This is to be noted that Trp 94, one of the three Trp residues present in Barnase, has been found to be solely responsible for a similar negative peak at 231 nm.[44] However, the intensity at 216 nm has been found to be identical for both the WT and W26F mutant, suggesting no significant loss of the secondary structure of the protein as a result of the site-directed mutagenesis.

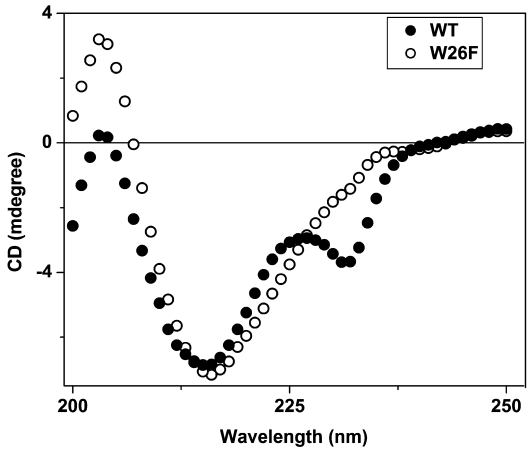

Figure 2. Far UV CD spectra of WT (filled circle) and W26F (empty circle) MPT63 at 298 K in 20 mM sodium phosphate buffer pH 7.5.

3.2. Steady State and Time Resolved Fluorescence Measurements of the WT and W26F Mutant. Figure 3(A) shows the fluorescence spectra of WT and W26F mutant at 298 K in 20 mM sodium phosphate buffer (pH 7.5) using λ_{exc} = 295 nm. While the emission maxima (λ_{max}) remain the same in both of the proteins (Table 1), the emission intensity of the W26F mutant has been found to be less than that of WT under the same experimental conditions (φ values shown in Table 1). This implies that Trp 26 contributes to the total fluorescence of the WT. The observation of identical λ_{max} for both WT and W26F mutant (330 nm) suggests that the mutation does not perturb the average Trp environment of the protein. This data along with far UV CD spectroscopy essentially establish relatively conservative nature of the W26F mutant.

Figure 3A inset also displays the emission spectra for WT at different λ_{exc}. The value of emission maxima (λ_{max}) and the shape of the emission spectra are found to be almost independent of λ_{exc} in the range 280 to 305 nm (Figure 3A Inset). The value of the λ_{max} observed for both the WT and the W26F are indicative of relatively less polar and more hydrophobic environment of the emitting Trp residues.

dx.doi.org/10.1021/jp307526f | J. Phys. Chem. B 2012, 116, 12489−12500

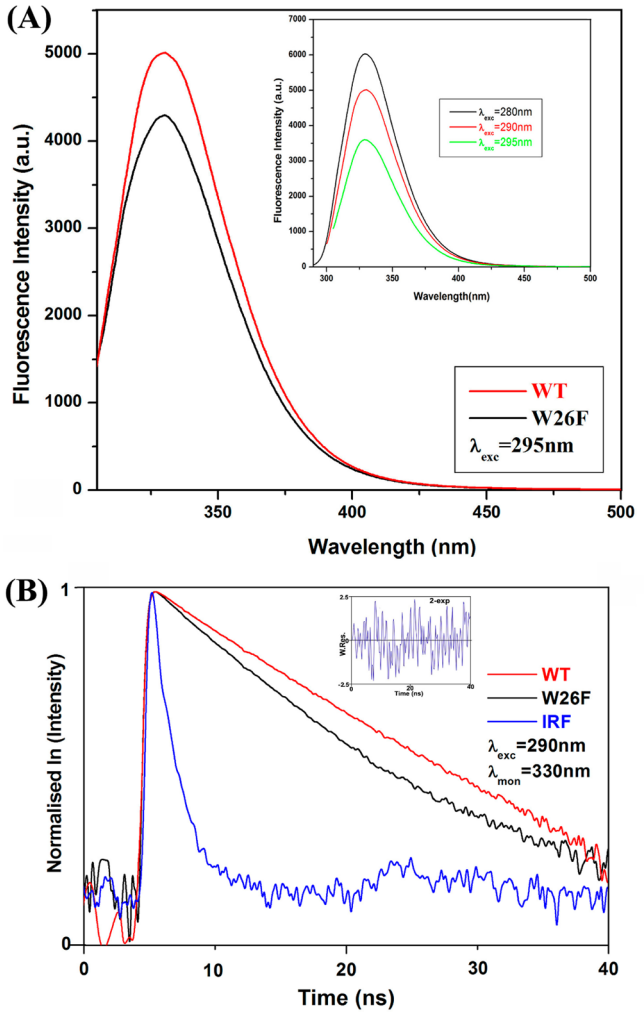

Figure 3. (A) Fluorescence spectra of WT and W26F MPT63 at 298 K. Excitation wavelength = 295 nm; [The inset shows the fluorescence spectra of WT at 298 K with excitation wavelength = 280 nm, 290 nm, 295 nm] excitation and emission band-pass = 10 and 5 nm, respectively, the concentration of protein used was 1 μM. (B) Fluorescence decay of 1 μM WT and W26F MPT63 in 20 mM sodium phosphate buffer pH 7.5, λ_{exc}=290 nm (LED), $\lambda_{monitor}$ = 330 nm (the excitation and emission band passes are 10 nm each).

The time-resolved fluorescence decay measurements of WT and W26F at 298 K using λ_{exc} = 290 nm are shown in Figure 3(B). The decay in both of the cases fit satisfactorily to a sum of two components (Table 1). The goodness of the fit has been established by randomness of the residual distribution. The addition of a third component does not improve the quality of the fit. Although the short lifetime component (1.5 ns) in WT does not change much due to mutation (1.6 ns observed in W26F), its amplitude is found to be larger in the mutant (Table 1). The long lifetime component (4.46 ns) for WT, however, decreases by approximately 20% in the case of the mutant protein (3.54 ns) with a decrease in the amplitude. The overall effect leads to a decrease in the average lifetime (τ_{av}) in W26F mutant compared to WT. A comparison has been made between the ratio of quantum yield observed with WT and that of the mutant with the ratio of their corresponding average lifetime values. It has been observed that the value of the ratio of φ is 1.11,whereas that of τ_{av} is 1.34.

3.3. Optical Resolution of All Four Trp Residues: Phosphorescence Spectra at 77 K. The LTP of WT is shown in Figure 4(A) with λ_{exc} = 280 nm. The overlapping phosphorescence spectra exhibit four (0,0) vibronic bands at 407, 412.2, 417.4, and 421.6 nm (Table 2). The band at 407 nm appears as a prominent shoulder and the band at 421.6 nm is much weaker compared to the bands at 412.2 and 417.4 nm [Figure 4(A)]. The band at 412.2 nm shows the maximum intensity with λ_{exc} = 280 nm. The intensity ratio of 412.2 and 417.4 nm bands is 1.26 with λ_{exc} = 280 nm (Table 2).

3.4. Assignments of the Four (0,0) Bands to Four Trp Residues. Using the crystal structure of MPT63 (Figure 1), we calculated the ASA values of all four Trp residues in MPT63 (Table 3). Phosphorescence (0,0) band in the blue side refers solvent exposed Trp residue with polar environment whereas (0,0) band in the longer wavelength corresponds to more rigid, hydrophobic and less solvent exposed Trp residues.[10] Local charges arising from charged residue (internal stark effect) also control the position of the (0,0) band.[5,10] The criteria of solvent exposure and the nature of immediate environment of each Trp residue (see Section 3.8) almost unambiguously indicate that the 407 nm band arises from Trp 82 (exposed, 60.2% accessible) and 412.2 nm band from Trp 48 (partially exposed, 12.4% accessible) (Table 3). Since ASA of both Trp 26 and Trp 129 are close to zero, the phosphorescence (0,0) bands of Trp 26 and Trp 129 should be red-shifted compared to those of Trp 82 and Trp 48. Thus, although it is clear that the two other (0,0) bands at 417.4 and 421.6 nm arise from Trp 26 and Trp 129, it is not possible to assign the (0,0) bands to a particular Trp residue. To solve the problem and assign these bands unambiguously, we have studied the phosphorescence of W26F mutant. Our attempt to purify the W129F mutant failed because of its expression predominantly in an inclusion body. Figure 4(A) reports the phosphorescence spectra of W26F at 77 K under similar experimental conditions. The presence of the first three bands at the same position and the absence of a 421.6 nm band clearly demonstrates that the 417.4 nm band arises from the Trp 129 and 421.6 nm band from Trp 26 in the phosphorescence spectra of the WT (Table 2). Figure 4(B) shows the deconvolution of the phosphorescence spectra of both the WT and W26F in the region 400 to 425 nm. The deconvoluted spectra clearly show the existence of four distinct (0,0) bands in the case of WT and three distinct (0,0) bands in the mutant W26F. The position of all three bands in W26F remains within 0.4 nm from that of WT [Figure

Table 1. Fluorescence Characteristics of MPT63 (WT) and It's Single Mutant (W26F) in Aqueous Buffer (pH 7.5) at 298 K[a]

system (in pH 7.5)	λ_{max} (nm)	quantum yield (ϕ)	singlet state lifetime monitoring the λ_{max}				rotational correlation time (θ_c) (ns) monitoring the λ_{max}
			τ_1 (ns)	τ_2 (ns)	τ_{av} (ns)	χ^2	
WT	330	0.232	1.49 (19.83%)	4.46 (80.17%)	3.87	1.025	6.8
W26F	330	0.208	1.57 (32.82%)	3.54 (67.18%)	2.89	0.959	6.5

[a] λ_{exc} = 290 nm. Concentration of protein in each case =1μM.

dx.doi.org/10.1021/jp307526f | J. Phys. Chem. B 2012, 116, 12489−12500

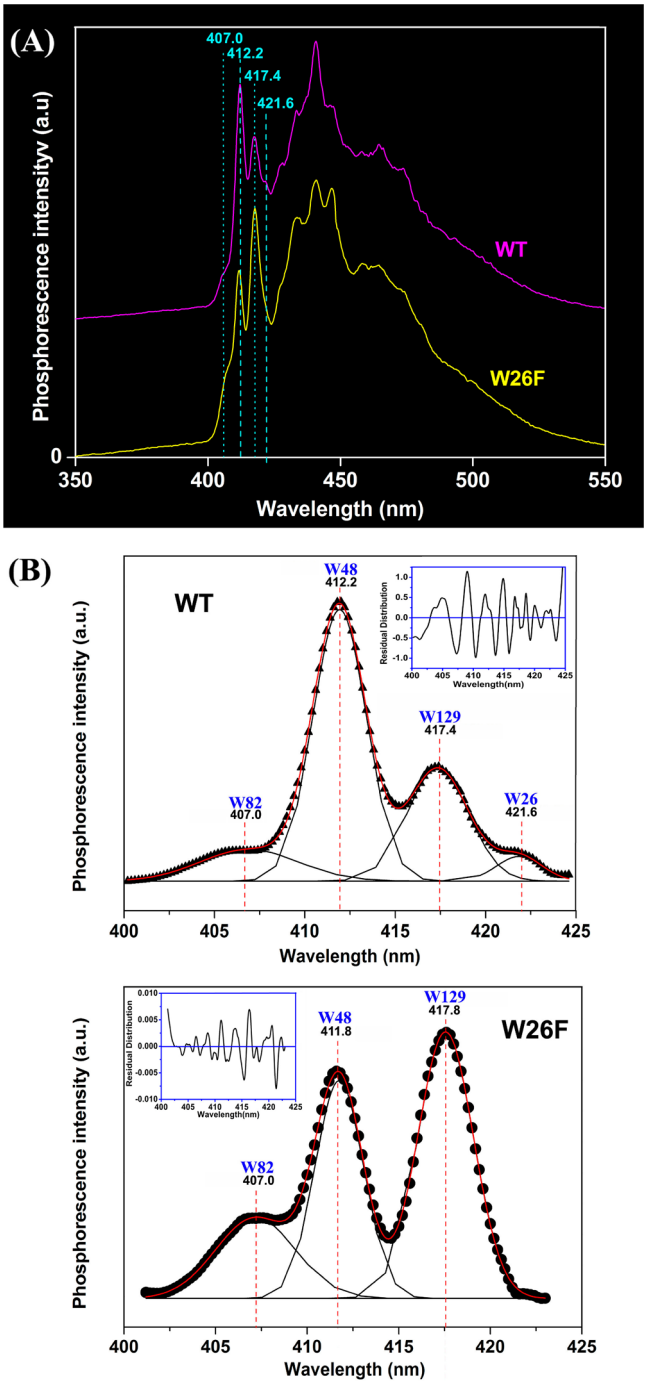

Figure 4. (A) Phosphorescence spectra of 5 μM WT and 5 μM W26F MPT63 in aq buffer +40% EG matrix at 77 K, λ_{exc} = 280 nm. Excitation and emission band-pass = 10 nm and 1 nm, respectively. (B) Deconvoluted phosphorescence spectra of WT and W26F at 77 K in the region from 400 to 430 nm.

4(A), Table 2].The intensity ratio of the (0,0) bands of Trp 48 and Trp 129 in the WT and the mutant are found to be reversed at λ_{exc} = 280 nm (Table 2).

3.5. Calculation of Intramolecular Trp−Trp Energy Transfer Efficiency (Singlet−Singlet Non Radiative) in WT and W26F. In order to explain the overall phosphorescence pattern of the different (0,0) bands in WT and W26F, we carried out a detailed intramolecular S↔S nonradiative ET efficiency calculation between different Trp pairs. The singlet−singlet nonradiative energy transfer efficiencies are calculated using Förster dipole−dipole ET mechanism[45]between Trp residues are given by the following:

$$E = R_0^6/(R^6 + R_0^6) \tag{3}$$

where R represents the Trp-Trp distance and R_0 is given by the following:

$$R_0 = (9.79 \times 10^3)(\kappa^2 n^{-4} \varphi_F J_{AD})^{1/6} \text{Å} \tag{4}$$

where J_{AD} denotes the spectral overlap integral, n is the refractive index of the medium, κ^2 is the dipole−dipole orientation factor, and φ_F is the donor fluorescence quantum yield in the absence of acceptor. κ^2 for each Trp-Trp pair is given by the following:

$$\kappa^2 = (\cos\theta_t - \cos\theta_D \cos\theta_A)^2 \tag{5}$$

where θ_t is the angle between the donor and acceptor dipole vectors and θ_D and θ_A are the angles between the direction vector and the donor and acceptor transition dipole vectors, respectively. κ^2 values were calculated for all possible combinations for the transition ($^1L_a \leftrightarrow {}^1L_a$, $^1L_a \leftrightarrow {}^1L_b$, $^1L_b \leftrightarrow {}^1L_a$, $^1L_b \leftrightarrow {}^1L_b$) between all Trp-Trp pairs following Desie et al. and Saha Sardar et al.[46,47] assuming the transition moment direction of ^1L_b makes an angle of 54° to the long axis of the indole molecule, while that of ^1L_a lies at an angle of −38° to the same axis.[48]

The ET efficiencies for various Trp pairs and the distance between Trp pairs are shown in Table 4 and Figure 5. The short Trp129−Trp26 distance (= 7.6 Å) is a clear indication of efficient ET between these two as reflected in the calculation. As expected, the ET efficiency is found to be close to unity (Table 4). The weak intensity of Trp 26 implies back ET from Trp 26 to Trp 129 is dominant. The low ET efficiency between Trp48 to Trp26 could also be assumed to account for very weak intensity of Trp26. From the calculation (Table 4), it is also predicted that Trp 82 transfers energy to both Trp 48 and Trp 129, whereas ET efficiency between Trp 48 and Trp129 is much less dominant. This justifies the observation of relatively stronger intensity for both Trp 48 and Trp 129. The observation of the weak shoulder for Trp 82 is reflected in relatively efficient ET to all other Trp residues (Table 4). The assumptions made in the calculations are as follows:

(i) There is no intermolecular S ↔ S nonradiative ET. The absence of intermolecular ET is assured by taking very dilute solution of the proteins.

(ii) The distance and orientation of each Trp with respect to every other Trp as obtained from crystal structure data remain the same in the frozen 40% EG glassy matrix at 77 K. Since the Trp 48 and Trp 129 are only 7 Å apart, a possibility of T ↔ T ET between them following Dexter's exchange mechanism cannot be ruled out.

The phosphorescence spectra also reveal the following:

(i) The contribution of solvent exposed Trp 82 to the total phosphorescence is very small due to efficient ET to other Trp residues. This is also reflected in the fluorescence spectra of both WT and W26F which show the λ_{max} of 330 nm. The contribution of a solvent exposed residue should have resulted in a more red-shifted fluorescence maximum.

(ii) The width of the phosphorescence (0,0) band measured for Trp 48 and Trp 129 (Table 2) shows that Trp48 is in

dx.doi.org/10.1021/jp307526f | J. Phys. Chem. B 2012, 116, 12489−12500

Table 2. Phosphorescence Data for WT and W26F MPT63 in a 40% Ethylene Glycol Matrix at 77 K (λ_{exc} = 280 nm)

system	position of the (0,0) Band (nm)[a]	width of the (0,0) band at half maxima (cm^{-1})[b]	phosphorescence lifetime (in sec) at 77 K monitoring (0,0) band				assignment of (0,0) band	[c]ratio of I_{W48} and I_{W129}
			τ_1 (s)	τ_2 (s)	τ_{av} (s)	χ^2		
WT	407.0 (Sh)		2.8 (97.4%)	6.4 (2.58%)	2.9	1.01	Trp82	1.23[d]
	412.2	141	6.4 (100%)		6.4	1.12	Trp48	1.26[e]
	417.4	160	5.9 (100%)		5.9	0.99	Trp129	1.17[f]
								1.02[g]
								0.74[h]
			4.1 (72.7%)	6.4 (27.3%)	4.7	1.03		
	421.6						Trp26	
W26F	407.0 (Sh)		3.4 (80.0%)	6.3 (20.0%)	4.0	0.97	Trp82	0.76[d]
	411.8	141	6.3 (100%)		6.3	1.06	Trp48	0.74[e]
								0.59[f]
	417.8	218	5.7 (100%)		5.7	0.97	Trp129	0.34[g]
			4.4 (61.6%)	6.3 (38.4%)	5.1	0.95		0.00[h]

[a]Error is ±0.2 nm. [b]Calculated from deconvoluted spectra (error= ± 5 cm^{-1}). [c]Intensity ratio of the (0,0) bands at 412.2 nm and 417.4 nm. [d]λ_{exc}= 270 nm. [e]λ_{exc} = 280 nm. [f]λ_{exc} = 295 nm. [g]λ_{exc} = 300 nm. [h]λ_{exc} = 305 nm.

Table 3. Accessible Surface Areas (in Å^2) for Each Trp Residue in WT and W26F MPT63

Trp residue	WT		W26F	
	ASA (Å^2)	% accessibility	ASA (Å^2)	% accessibilty
W26	4.3	1.7		
W48	31.0	12.4	31.0	12.4
W82	149.8	60.2	137.9	55.4
W129	0	0	0	0

Table 4. Intramolecular Trp-Trp Energy Transfer Efficiencies and Inter-Trp Distances (in Å) in WT and W26F MPT63

Trp residues of WT (donor–acceptor)	intramolecular Trp-Trp energy transfer efficiencies				distance (Å)[a]
	$^1L_a \rightarrow {}^1L_a$	$^1L_a \rightarrow {}^1L_b$	$^1L_b \rightarrow {}^1L_a$	$^1L_b \rightarrow {}^1L_b$	
W82↔W48	0.82	0.88	0.69	0.80	18.89
W82↔W129	0.95	0.42	0.00	0.73	18.32
W82↔W26	0.74	0.35	0.58	0.85	14.61
W48↔W129	0.87	0.50	0.91	0.16	16.06
W48↔W26	0.22	0.70	0.14	0.24	19.57
W129↔W26	0.99	0.99	0.98	0.99	7.64
Trp residues of W26F (donor–acceptor)	intramolecular Trp-Trp energy transfer efficiencies				distance (Å)[a]
	$^1L_a \rightarrow {}^1L_a$	$^1L_a \rightarrow {}^1L_b$	$^1L_b \rightarrow {}^1L_a$	$^1L_b \rightarrow {}^1L_b$	
W82↔W48	0.82	0.34	0.93	0.17	18.02
W82↔W129	0.78	0.20	0.77	0.10	18.13
W48↔W129	0.86	0.47	0.90	0.43	16.03

[a]Distances are from the center of mass of the adjacent double bond of the nitrogen atom of the indole moiety of Trp residues.

somewhat more homogeneous environment compared to Trp 129 particularly in the mutant W26F.

3.6. Trp 129 in the WT and W26F Mutant Could be Selectively Excited Using λ_{exc} of 305 nm: Phosphorescence Spectra at Different Excitation Wavelengths. The phosphorescence spectra of WT and W26F mutant as a function of λ_{exc} from 270 nm to 305 nm at 77 K are shown in Figure 6 .The intensity ratio of Trp 48 and Trp 129 changes dramatically as one moves from λ_{exc} = 270 nm to λ_{exc} = 305 nm for both the WT and the W26F (Figure 6, Table 2). For WT,

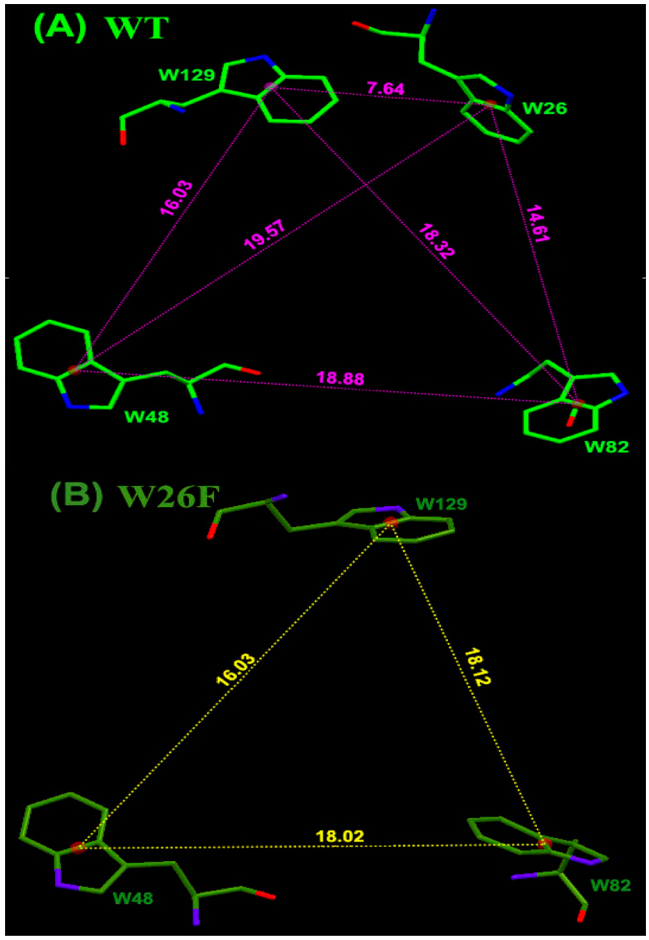

Figure 5. Orientations and distances of different Trp residues with respect to each other in (A) WT and (B) W26F MPT63.

the (0,0) band of Trp 48 appears as the strongest band at λ_{exc} = 280 nm but becomes very weak at λ_{exc} = 305 nm [Figure 6(A)]. At λ_{exc} = 300 nm, the intensity of the (0,0) bands of Trp 48 and Trp 129 are found to be same for WT [Figure 6(A), Table 2]. For W26F, the intensity of Trp 48 is found to be less than that of the Trp 129 band for all of the excitation wavelength. At λ_{exc} = 305 nm, the LTP spectra show only the band of Trp 129 and

dx.doi.org/10.1021/jp307526f | J. Phys. Chem. B 2012, 116, 12489–12500

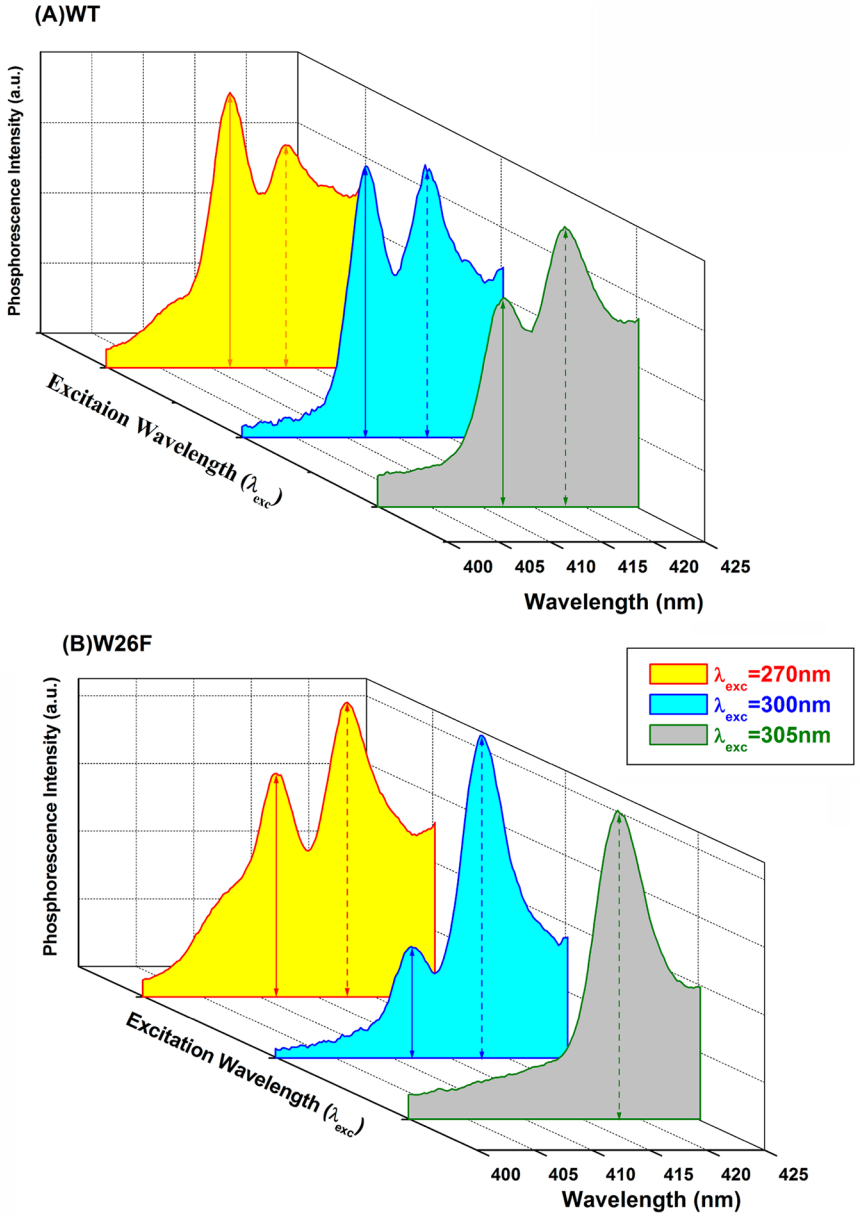

Figure 6. Phosphorescence spectra of (A)WT and (B)W26F in aqueous buffer +40% EG matrix at 77 K with different excitation wavelength. Protein concentration 5 μM, excitation bandpass = 10 nm and emission bandpass = 1 nm in each case except with λ_{exc} = 305 nm, where the emission band-pass = 2.5 nm.

the corresponding band for Trp 48 disappears completely [Figure 6(B)]. At low energy excitations (λ_{exc} = 295−305 nm) the weak band of Trp 82 also disappears for both the WT and the W26F (Figure 6). The intensity pattern observed for Trp 48 and Trp 129 as a function of excitation wavelength is consistent with the more buried and rigid nature of the environment Trp129 compared to that of Trp 48 which is partially solvent exposed. The weak band of Trp 26 in WT is not observed at higher excitation wavelength (λ_{exc} = 305 nm) possibly due to the masking effect of strong Trp 129 band [Figure 6(A)]. Furthermore, we used emission band-pass = 2.5 nm for λ_{exc} = 305 nm since the absorbance of the protein at 305 nm is very weak (Figure 6). The result suggests that Trp 129 could be selectively excited at λ_{exc} = 305 nm.

3.7. Phosphorescence Decay at 77 K. The phosphorescence decay was measured by monitoring the (0,0) vibronic bands at 407 nm (Trp 82), 412 nm (Trp 48), and 418 nm (Trp 129) for both the WT and W26F mutant at 77 K using λ_{exc} = 280 nm. For Trp 48, the decay profile was fit to a single exponential. Since the prominent shoulder at 407 nm for Trp 82 is on the rising part of the (0,0) band of Trp 48 at 412.2 nm, the decay profiles for Trp 82 for the WT and the mutant were fit to a sum of two exponentials keeping one component fixed at a phosphorescence lifetime (τ_p) of Trp 48 (Table 2). For Trp 129, the decay profiles for both proteins were fit to a single exponential and also to a sum of two exponentials keeping one component fixed at τ_p of Trp 48 assuming a slight underlying contribution from Trp 48. All of the recovered lifetime along with χ^2 values are provided in Table 2. Although Trp 48 and Trp 129 behave as normal Trp residues in proteins exhibiting a lifetime of 6 to 5 s, Trp 82 shows shorter τ_p of 2.9 and 4.0 s in the WT and in the mutant, respectively. The shorter τ_p for Trp 82 is a definite indication of a quenched Trp residue. The values of τ_p thus support our ET efficiency calculation showing

dx.doi.org/10.1021/jp307526f | J. Phys. Chem. B 2012, 116, 12489−12500

Table 5. Different Residues within 5 Å from the Tryptophan Residues in WT and W26F MPT63[a]

position of tryptophans of WT	residues within 5 Å radius	
	non polar residues	polar residues
W26	**Leu13** (2.8, 2.9), Met15, Leu24, Gly25, Val28, Ala52, Val54, Pro63, Ala64, Val65, Phe68, Ile90,Met119, Leu127, Trp129	Ser11, Glu12, Lys27, Thr53, Asn55, Gln67
W48	Leu31, Val47, Ala50, Ile105, Tyr106,**Phe107**(3.0, 2.9), Val109, Pro114	Lys32, Ser33, Ser34, Gln46, Glu49, Ser113
W82	**Val80** (3.0), Leu81, Ala84	Ser66, Arg79, Gln83
W129	Gly7, Leu9, Gly10, Leu13, Trp26,Val28, Phe68, Ile116, **Val117** (2.9, 2.9), Ala118, Met119, Leu127, Ile128, Pro131	Lys8, **Ser11** (3.0), Glu12, Lys27, Thr115,, Glu130
position of tryptophans of W26F	residues within 5 Å radius	
	non-polar residues	polar residues
W48	Leu31, Val47, Ala50, Ile105, Tyr106, **Phe107** (2.9, 3.0), Val109, Pro114	Lys32, Ser33, Ser34, Gln46, Glu49, Ser113, Thr115
W82	**Val80** (3.1), Leu81, Ala84	Ser66, Arg79, Gln83
W129	Gly7, Leu9, Gly10, Leu13, Phe26, Val28, Phe68, Ile116, **Val117** (2.9, 2.9), Ala118, Met119, Leu127, Ile128, Pro131	Lys8, **Ser11**(3.0), Glu12, Lys27, Thr115, Glu130

[a]Trp residue makes polar contacts with the bold amino acid residues. Values in parentheses are the polar contacts distances in Å. See text for measurement.

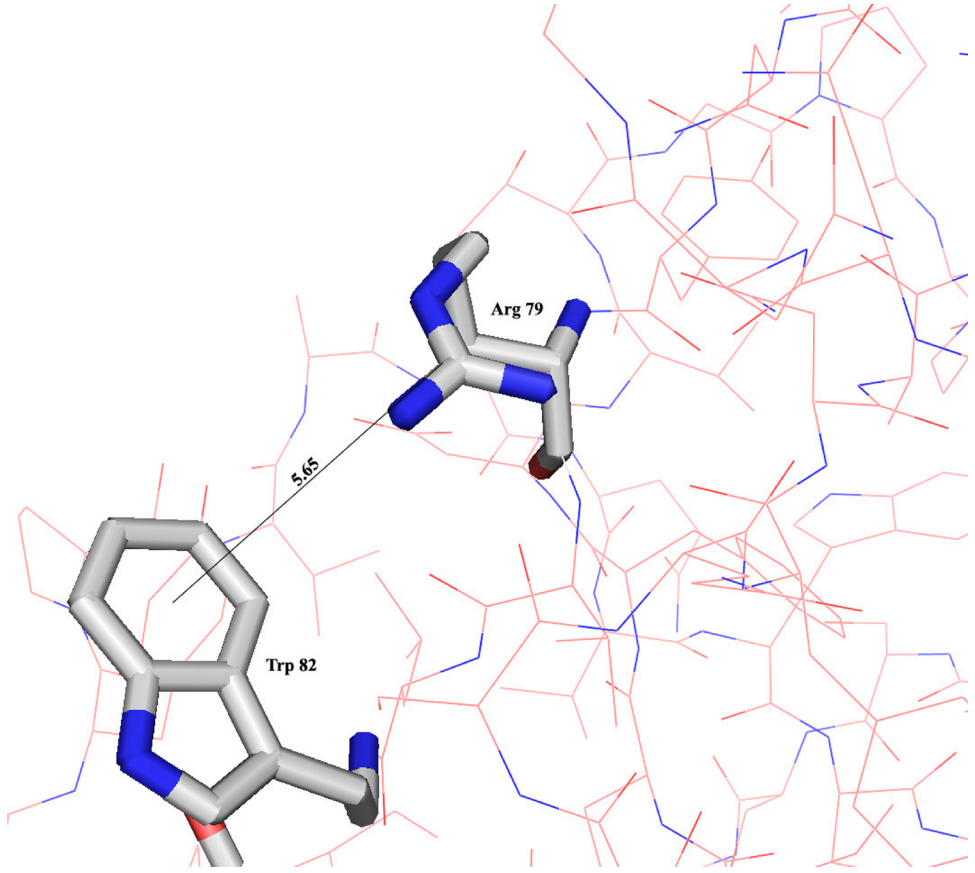

Figure 7. The proximity between Arg79 and Trp82.

that Trp 82 efficiently transfers energy to other Trps. The decay at the 421.6 nm band for Trp 26 with narrow band-pass was found to be too noisy to be analyzed properly, since the analysis needs fitting with a sum of several exponentials.

3.8. Environments of Trp Residues in WT and in W26F. Table 5 shows different amino acid residues which are present within 5 Å of each Trp in WT and in W26F mutant. The distances are calculated from the center of mass of the adjacent double bond of the nitrogen atom of the indole moiety of Trp residues using crystal structure for WT. For the mutant protein, a model structure generated using DISCOVERY STUDIO has been used for this purpose (Figure 1). It can be noted that Trp 26 and Trp 129 are surrounded by many nonpolar residues for the proteins. This observation, together with the calculated ASA values of Trp 26 and Trp 129 (Table 3) points out that these Trp residues are in a buried hydrophobic region. Trp 82, however, has been found to be surrounded by three nonpolar and three polar residues (Table 5). Particularly important is the presence of Arginine (Arg) 79, which is expected to create a more polar environment around Trp 82. Positively charged Arg 79 being located on the benzene side of the inole ring (Figure 7) could favorably interact with

dx.doi.org/10.1021/jp307526f | J. Phys. Chem. B 2012, 116, 12489−12500

the ^1L_a state.[49−53] Similarly, the residue Trp 48 is also surrounded by both polar and nonpolar residues and experiences a somewhat mixed environment (Table 5). The environments of the Trp residues are expected to be similar for the WT and W26F. This is because both the secondary structure (far UV CD) and the average Trp environments (monitored by steady state and time-resolved fluorescence) show similar behavior for both proteins. This has been further confirmed by the phosphorescence spectroscopy described above.

The intensity ratio of the (0,0) bands of Trp 48 and Trp 129 in the WT and in the mutant [Figure 4(A) and Table 2] are found to be reversed at λ_{exc} = 280 nm. This is indicative of subtle change of microenvironment of Trp 48 and Trp 129 resulting in larger value of $^1L_b \leftrightarrow {}^1L_b$ ET between them. Since the distance between Trp 48 and Trp 129 in the mutant is unaltered, the results imply that orientation with respect to each other is slightly changed leading to a difference in ET efficiency (Table 4).

3.9. Tyrosine Residues in MPT63 are Silent upon Excitation. MPT63 contains four Tyr residues (Tyr 3, Tyr 41, Tyr 78, and Tyr 106). However, they do not contribute to the total phosphorescence of either WT or W26F. This is evident from the absence of any underlying broad background in the region of 350−400 nm of the phosphorescence spectra for both proteins[54] using λ_{exc} = 280 nm or 270 nm, which could excite the Tyr residue. These results indicate that Tyr residues either transfer energy efficiently at the singlet level to other Trp residues or they are intrinsically quenched by nearby amino acid residues. The distances of different Tyr residues with respect to Trp residues given in Table 6 are within the distance of Förster's ET mechanism. Furthermore, a close look at the environments of Tyr residues in MPT63 reveals that Arg 71 and Arg 79 are within 5 Å of Tyr 78 and Tyr 106, respectively. The electric field of charged Arg has been shown to quench the Tyr emission by fast electron transfer process.[49−53]

Table 6. Tyr-Trp Distances (in Å) in WT and W26F MPT63[a]

WT	Trp26	Trp48	Trp82	Trp129
Tyr 3	10.93	28.94 (28.90)	21.53 (22.50)	13.53 (13.50)
Tyr41	21.1	14.00 (14.0)	10.40 (8.70)	23.00 (23.00)
Tyr78	22.7	7.90 (7.90)	20.0 (18.70)	19.70 (19.70)
Tyr106	17.8	12.60 (12.60)	15.9 (16.00)	18.10 (18.10)

[a]The value within the bracket indicates the distance in W26F.

3.10. The Overall Motion of the Protein Revealed by Time Resolved Anisotropy. The time-resolved anisotropy decay monitoring λ_{max} of the WT using λ_{exc} = 290 nm is shown in Figure 8. The data have been fit to a single exponential function and the rotational correlation time recovered from the analysis is 6.8 ns (Table 1). The θ_c for the mutant W26F have also been measured under similar experimental conditions and θ_c is found to be 6.5 ns (Table 1).

For a globular protein, θ_c can be calculated using the following:

$$\theta = \frac{\eta M}{RT}(\nu + h) \tag{6}$$

where η is the viscosity of the solvent (0.94×10^{-3} Pas), M is the molecular weight in Dalton, ν is the partial specific volume of the protein (assuming 0.72 mL/g protein, and h is the degree of hydration (assuming 0.23 cm^3/g protein). The θ_c of a protein like MPT 63 having a molecular weight of about 17.5 kD calculated from eq 6 (6.4 ns) matches well with the experimental data (6.8 ns for WT MPT 63). Similar rotational correlation time (θ = 6.5 ns) has been obtained for the W26F mutant, which indicates that the mutation does not affect the overall hydrodynamic radius of the protein.

3.11. Significance of the Resolved Phosphorescence Spectra. Since Trp is an intrinsic fluorescence probe of a protein, it has been used extensively to monitor the conformation changes a protein experiences due to ligand binding or unfolding. However, because Trp fluorescence is inherently broad, site specific assignments of the individual Trp in a multi-Trp protein have been found to be almost impossible. Time-resolved fluorescence studies also offer limited help because even single Trp containing protein can show the existence of two or more lifetime components. There are several attempts that have been explored to assign the spectroscopic change of a single Trp so that the folding of a particular portion (or ligand binding of an individual domain) can be explored without using external fluorophores or

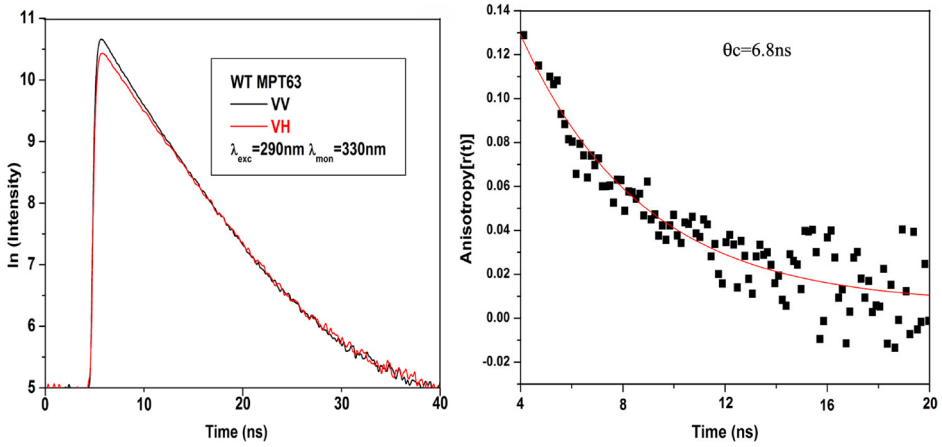

Figure 8. Fluorescence anisotropy decays of WT MPT63 (5 μM); I_{VV} and I_{VH} represent decays of emission of WT with an excitation polarizer at the vertical position and emission polarizer at the vertical and horizontal positions, respectively. λ_{exc}= 290 nm, λ_{mon}= 330 nm; excitation and emission band-pass = 10 nm each.

dx.doi.org/10.1021/jp307526f | J. Phys. Chem. B 2012, 116, 12489−12500

radiolabels. Notable examples include using DAS or using a quencher molecule to resolve different lifetime components. The use of site-specific mutagenesis has also been used in tandem with these photophysical explorations. One of the most successful techniques in this regard is the use of 19F NMR spectroscopy of 19F labeled Trp residues.[55−57] For example; 19F NMR spectroscopy with fluorine-labeled Trp has been used with IFABP and ADA to characterize unknown folding intermediates.[55,56] The same technique with PapD has been used to study the interactions between two domains of the protein.[57] These methods, while extremely sensitive and useful with many different proteins, require exhaustive molecular biology techniques and technical details of NMR. Additionally, NMR spectroscopy requires relatively high concentration (although with the use of cryoprobes, this is less of an issue nowadays) which could add aggregation-related problems. The phosphorescence method described here is rapid, less expensive, and requires micromolar concentration of protein. Experiments are underway in our laboratory to study the urea and pH-induced unfolding of MPT63 to explore how these different Trp residues behave as the protein unfolds.

4. CONCLUSIONS

The paper presents an unprecedented event of optical resolution of all four Trp residues (located at 26, 48, 82, and 129) in MPT63 protein by simple inexpensive phosphorescence spectroscopy at 77 K. The intrinsic delicate microenvironment of the Trp residues and their positions with respect to each other within the protein architecture are found to be responsible for such events. The assignment of each optically resolved (0,0) band of particular Trp residue is ascertained by using the phosphorescence spectra of the mutant W26F and the calculation of ASA and the microenvironment of each Trp residue and the intramolecular S ↔ S nonradiative ET efficiency between all of the Trp-pairs based on crystal structure data of the WT protein. The lowest triplet state energy (E_{T1}) of Trp residue in MPT63 is in the order: E_{T1}(W82) > E_{T1}(W48) > E_{T1}(W129) > E_{T1}(W26). This order is consistent with ASA values of Trp residues. Apart from solvent exposure, the presence of charged residue Arg 79 very near to solvent exposed Trp 82 may also be responsible for the highest energy (0,0) band of Trp 82 among all the Trp residues. The phosphorescence (0,0) band observed at 421.6 nm assigned for Trp 26 is found to be the longest wavelength (0,0) band so far reported in the literature. The ratio of the intensity of the different (0,0) bands depends markedly on the λ_{exc}. The results revealed that Trp129 could be almost selectively excited with λ_{exc} = 305 nm in WT and in W26F.

In contrast, fluorescence maxima is found to be independent of λ_{exc} for both WT and W26F. The λ_{max} and the time-resolved fluorescence in the WT and the mutant, however, indicate that the fluorescence of the WT is dominated by buried and partially exposed Trp residues, viz., Trp129, Trp26, and Trp48.

CD studies showed that the secondary structure is not altered due to mutation of Trp 26 by phenylalanine. θ_c of the WT and the W26F from time-resolved anisotropy decay confirms the globular nature of the protein and also suggests that the overall hydrodynamic radius remain intact in the mutant.

AUTHOR INFORMATION

Corresponding Author

* Tel.:+91-9836940620 (S.G.), +9133-2241 3893 (S.G.); Fax: +9133-2241 3893 (S.G.); E-mail: sanjibg@cal2.vsnl.net.in (S.G.); pchemsg@gmail.com (S.G.); E-mail: krish@iicb.res.in (K.C.).

Notes

The authors declare no competing financial interest.

ACKNOWLEDGMENTS

S.G. gratefully acknowledges DST, Govt. of India (SR/S1/PC-57/2008) and CSIR, Govt of India (21(0871)/11/EMR-II) for financially supporting this work. R.G. and M.M. thank CSIR and DST (No. SR/S1/PC-57/2008), respectively, for SRF fellowship. K.C. acknowledges CSIR for Network EMPOWER Project (OLP-004) grant from CSIR.

REFERENCES

(1) Wasylewski, Z.; Koloczek, H.; Wasniowska, A. *Eur. J. Biochem.* **1988**, *172*, 719−724.
(2) Lakowicz, J. R. *Principles of Fluorescence Spectroscopy*; Kluwer/Plenum Press: New York, 1999; Chapter 7.
(3) Hahn, D. K.; Callis, P. R. *J. Phys. Chem. A* **1997**, *101*, 2686−2691.
(4) Purkey, It. M.; Galley, W. C. *Biochemistry* **1970**, *9*, 3569−3575.
(5) Hershberger, M. V.; Maki, A. H.; Galley, W. C. *Biochemistry* **1980**, *19*, 2204−2209.
(6) Von Shutz, J. U.; Zuclich, J. A.; Maki, A. H. *J. Am. Chem. Soc.* **1974**, *96*, 714−718.
(7) Kwiram, A. L.; Ross, J. B. A. *Annu. Rev. Biophys. Bioeng.* **1982**, *11*, 223−249.
(8) Lam, W. C.; Maki, A. H.; Itoh, T.; Hakoshima, T. *Biochemistry* **1992**, *31*, 6751−6760.
(9) Mukhopadhyay, S.; Maity, S. S.; Roy, A.; Chattopadhyay, D.; Ghosh, K. S.; Dasgupta, S.; Ghosh, S. *Biochimie* **2010**, *92*, 136−146.
(10) Ozarowski, A.; Barry, J. K.; Matthews, K. S.; Maki, A. H. *Biochemistry* **1999**, *38*, 6715−6722.
(11) Callis, P. R.; Liu, T. *J. Phys. Chem. B* **2004**, *108*, 4248−4259.
(12) Ghosh, S.; Misra, A.; Ozarowski, A.; Stuart, C.; Maki, A. H. *Biochemistry* **2001**, *40*, 15024−15030.
(13) Ghosh, S.; Misra, A.; Ozarowski, A.; Maki, A. H. *J. Phys. Chem. B* **2003**, *107*, 11520−11526.
(14) Mukherjee, M.; Saha Sardar, P.; Ghorai, S.; Samanta, S.; Singha Roy, A.; Dasgupta, S.; Ghosh, S. *J. Photochem. Photobiol. B: Biol.* **2012**, *115*, 93−104.
(15) Li, Z.; Bruce, A.; Galley, W. C. *Biophys. J.* **1992**, *61*, 1364−1371.
(16) Eftink, M. R. In *AdVances in Biophysical Chemistry*; Bush, C. A., Ed.; JAI Press: Greenwich, CT, 1992; Vol. *2*, pp 81−114.
(17) Galley, W. C.; Williams, R. E.; Goodfriend, L. *Biochemistry* **1982**, *21*, 378−383.
(18) Davis, J. M.; Maki, A. H. *Biochemistry* **1984**, *23*, 6249−6256.
(19) Strambini, G. B.; Gabellieri, E. *Biochemistry* **1989**, *28*, 160−166.
(20) Ghosh, S.; Zang, L. H.; Maki, A. H. *J. Chem. Phys.* **1988**, *88*, 2769−2775.
(21) Zang, L. H.; Ghosh, S.; Maki, A. H. *Biochemistry* **1988**, *27*, 7820−7825.
(22) Zang, L. H.; Ghosh, S.; Maki, A. H. *Biophys. J.* **1988**, *53*, 2245−2251.
(23) Zang, L. H.; Ghosh, S.; Maki, A. H. *Biochemistry* **1989**, *28*, 2245−2251.
(24) Strambini, G. B.; Lehrer, S. S. *Eur. J. Biochem.* **1991**, *195*, 645−651.
(25) Bódis, E.; Strambini, G. B.; Gonnelli, M.; Csizmadia, A. M.; Somogyi, B. *Biophys. J.* **2004**, *87*, 1146−1154.
(26) Cioni, P.; Onuffer, J. J.; Strambini, G. B. *Eur. J. Biochem.* **1992**, *209*, 759−764.
(27) Cioni, P.; Puntoni, A.; Strambini, G. B. *Biophys. Chem.* **1993**, *46*, 47−55.

(28) Eftink, M. R.; Ramsay, G. D.; Burns, L.; Maki, A. H.; Mann, C. J.; Matthews, C. R.; Ghiron, C. A. *Biochemistry* **1993**, *32*, 9189−9198.
(29) Broos, J.; Strambini, G. B.; Gonnelli, M.; Vos, E. P. P.; Koolhof, M.; Robillard, G. T. *Biochemistry* **2000**, *39*, 10877−10883.
(30) D'Auria, S.; Varriale, A.; Gonnelli, M.; Saviano, M.; Staiano, M.; Rossi, M.; Strambini, G. B. *J. Proteome Res.* **2007**, *6*, 1306−1312.
(31) Saha Sardar, P.; Maity, S. S.; Ghosh, S.; Chatterjee, J.; Maiti, T. K.; Dasgupta, S. *J. Phys. Chem. B* **2006**, *110*, 21349−21356.
(32) Kerwin, B. A.; Aoki, K. H.; Gonelli, M.; Strambini, G. B. *Photochem. Photobiol.* **2008**, *84*, 1172−1181.
(33) D'Auria, S.; Staiano, M.; Varriale, A.; Gonnelli, M.; Marabotti, A.; Rossi, M.; Strambini, G. B. *J. Proteome Res.* **2008**, *7*, 1151−1158.
(34) D'Auria, S.; Aurilia, V.; Marabotti, A.; Gonnelli, M.; Strambini, G. B. *J. Phys. Chem. B* **2009**, *113*, 13171−13178.
(35) Galley, W.C. In *Concepts of Biochemical Fluorescence*; Chen, R. F., Edelhoch, H., Eds.; Marcel Dekker: New York, 1976; Vol. *2*, Chapter 8, pp 409−439.
(36) Goulding, C. W.; Parseghian, A.; Sawaya, M. R.; Cascio, D.; Apostol, M. I.; Gennaro, M. L.; Eisenberg, D. *Protein Sci.* **2002**, *11*, 2887−2893.
(37) Manca, C.; Lyashchenko, K.; Wiker, H. G.; Usai, D.; Colangeli, R.; Gennaro, M. L. *Infect. Immun.* **1997**, *65*, 16−23.
(38) Callis, P. R. *Methods Enzymol.* **1997**, *278*, 113−150.
(39) Demas, J. N.; Crosby, G. A *J. Phys. Chem.* **1971**, *75*, 991−1024.
(40) *FELIX 32, Operation Manual, Version 1.1*; Photon Technology International, Inc.: Lawrenceville, NJ, 2003.
(41) DeLano, W. L. *The PyMOL Molecular Graphics System*; DeLano Scientific: San Carlos, CA, 2004; http://www.pymol.sourceforge.net.
(42) Hubbard, S. J.; Thornton, J. M. *'NACCESS' Computer Program, Department of Biochemistry and Molecular Biology*; University College: London, 1993.
(43) Rucker, A. L.; Pager, C. T.; Campbell, M. N.; Qualls, J. E.; Creamer, T. P. *Proteins* **2003**, *53*, 68−75.
(44) Vuilleumier, S.; Sancxho, J.; Loewenthal, R.; Fersht, A. R. *Biochemistry* **1993**, *32*, 10303−10313.
(45) (a) Förster, T. Zwischenmolekulare energiewanderung und fluoreszenz. *Ann. Phys. (Leipzig)* **1948**, *2*, 55−75. (b) Förster, T. *Discuss.Faraday Soc.* **1959**, *27*, 7−17.
(46) Desie, G.; Boens, N.; De Schryver, F. C. *Biochemistry* **1986**, *25*, 8301−8308.
(47) Saha Sardar, P.; Maity, S. S.; Das, L.; Ghosh, S. *Biochemistry* **2007**, *46*, 14544−14556.
(48) Yamamoto, Y.; Tanaka, J. *Bull. Chem. Soc. Jpn.* **1972**, *45*, 1362−1366.
(49) Harvey, B. J.; Bell, E.; Brancaleon, L. *J. Phys. Chem. B* **2007**, *111*, 2610−2620.
(50) Vivian, J. T.; Callis, P. R. *Biophys. J.* **2001**, *80*, 2093−2109.
(51) Samanta, U.; Pal, D.; Chakrabarti, P. *Proteins* **2000**, *38*, 288−300.
(52) Nanda, V.; Brand, L. *Proteins* **2000**, *40*, 112−125.
(53) Koenig, S.; Muller, L.; Smith, D. K. *Chem.—Eur. J.* **2001**, *7*, 979−986.
(54) Ghosh, S.; Zang, L. H.; Maki, A. H. *Biochemistry* **1988**, *27*, 7816−7820.
(55) Ropson, I. J.; Frieden, C. *Proc. Natl. Acad. Sci, U.S.A.* **1992**, *89*, 7222−7226.
(56) Shu, Q.; Frieden, C. *Biochemistry* **2004**, *43*, 1432−1439.
(57) Bann, J. G.; Pinkner, J.; Hultgren, S. J.; Frieden, C. *Proc. Natl. Acad. Sci, U.S.A.* **2002**, *99*, 709−714.